GEOPHYSICS, VOL. 71, NO. 3 (MAY-JUNE 2006); P. D45–D58, 7 FIGS.
10.1190/1.2194520

Weak elastic anisotropy by perturbation theory

Vigen Ohanian[1], Thomas M. Snyder[2], and José M. Carcione[3]

ABSTRACT

We demonstrate the advantages of adopting a wave-vector-based coordinate system (WCS) for the application of perturbation theory to derive and display approximate expressions for qP- and qS-wave polarization vectors, phase velocities, and group velocities in general weakly anisotropic media. The advantages stem from two important properties of the Christoffel equation when expressed in the WCS: (1) Each element of the Christoffel matrix is identical to a specific stiffness component in the WCS, and (2) the Christoffel matrix of an isotropic medium is diagonal in the WCS.

Using these properties, one can easily identify the small components of the Christoffel matrix in the WCS for a weakly anisotropic medium. Approximate solutions to the Christoffel equation are then obtained by straightforward algebraic manipulations, which make our perturbation theory solution considerably simpler than previously published methods. We compare and contrast our solutions with those discussed by other workers. Numerical comparisons between the exact, first-order, and zero-order qS-wave polarization vectors illustrate the accuracy of our approximate formulas. The form of the WCS phase-velocity expressions facilitates the derivation of closed-form, first-order expressions for qP- and qS-wave group-velocity vectors, providing explicit formulas for the direction of propagation of seismic energy in general weakly anisotropic media. Numerical evaluation of our group-velocity expressions demonstrates their accuracy.

We discuss problems with the approximate qS-wave group velocities and polarizations in neighboring directions of singularities. Standard methods are used to transform our solutions from the WCS to the acquisition coordinates, as illustrated by application to orthorhombic symmetry.

INTRODUCTION

The physical properties of elastic waves propagating in linear nondissipative elastic media are characterized by P- and S-wave polarization vectors, phase velocities, and group velocities. These wave attributes arise from the solutions of the Christoffel equation. Numerical modeling of elastic waves propagating in anisotropic media of arbitrary symmetry (triclinic) can be computer intensive (Igel et al., 1991). In view of the ubiquity of weak anisotropy in the earth's crust and robust applicability of first-order solutions to the Christoffel equation, there has been longstanding interest in developing approximate solutions for weak elastic anisotropy problems (Thomsen, 1986; Mensch and Rasolofosaon, 1997; Pšenčík and Gajewski, 1998). Closed-form approximate wave-attribute expressions also provide physical insight into elastic anisotropy that is otherwise not afforded by numerical solutions.

Several authors have obtained approximate solutions to the Christoffel equation by linearizing its exact solutions. Thomsen (1986), using Taylor series expansions of the exact vertical transverse isotropy (VTI) formulas, obtains first-order expressions for qP- and qS-waves in weak VTI media. Rommel (1994) uses a similar approach to derive first-order expressions for polarization vectors for weak VTI systems. Ohanian et al. (2002) use a set of coordinate transformation rules to derive first-order qP- and qS-wave attribute expressions for weak horizontal transversely isotropic (HTI) media directly from the corresponding VTI expressions. Sayers (1994) uses an expansion into spherical harmonics to obtain approximate relations for phase velocity of qP-waves in arbitrary weakly anisotropic media. Tsvankin (1997) develops the approximate phase-velocity equation for qP-waves in orthorhombic media by linearizing the corresponding exact equations.

Perturbation theory offers a different approach for computing approximate solutions of the Christoffel equation, in that it makes no reference to the exact solutions of the equation. Backus (1965),

Manuscript received by the Editor September 19, 2002; revised manuscript received October 17, 2005; published online May 25, 2006.
[1]ENSCO, Inc., 5400 Port Royal Road, Springfield, Virginia 22151-2312. E-mail: ohanian.vigen@ensco.com.
[2]Lincoln Land Community College, Department of Mathematics and Engineering Sciences, 5250 Shepherd Road, Springfield, Illinois 62794-9256. E-mail: tom.snyder@llcc.edu.
[3]Istituto Nazionale di Oceanografia e di Geofisica Sperimentale (OGS), Borgo Grotta Gigante 42c, 34010 Sgonico, Trieste, Italy. E-mail: jcarcione@ogs.trieste.it.

in dealing with refraction shooting in nearly isotropic media, uses perturbation theory to obtain information about the azimuthal dependence of qP- and qS-wave phase velocities for horizontal propagation. Jech and Pšenčík (1989) use first-order perturbation theory to obtain expressions for phase velocities and polarization directions for qP- and qS-waves in general weakly anisotropic media. Corrections to their qS-wave polarization expressions are given by Thomson et al. (1992). Gajewski and Pšenčík (1996) and Pšenčík and Gajewski (1998) use perturbation theory to obtain first-order expressions for qP-wave phase velocities and polarizations in weakly anisotropic media with applications to media with VTI, HTI, and orthorhombic symmetry. Ohanian (1996) uses perturbation theory to investigate phase velocities and polarization vectors for waves in weak VTI systems. Mensch and Rasolofosaon (1997) apply the perturbation approach to obtain approximate qP- and qS-wave phase-velocity expressions for arbitrary anisotropy.

The analysis of the Christoffel equation is simplified substantially when it is transformed to a wave-vector coordinate system (WCS). This Cartesian coordinate system has one of its axes in the direction of the wave vector. For a given wave-propagation direction, we demonstrate that the general solutions of the Christoffel equation are expressible in terms of only six independent stiffness components of the WCS. Moreover, for an isotropic medium, the Christoffel matrix in the WCS is strictly diagonal. These simplifications make the WCS a convenient coordinate system for the application of perturbation theory to the weak anisotropy problem. Mensch and Rasolofosaon (1997) obtain their qP- and qS-wave phase velocity expressions in the WCS.

In continuation of previously cited works, we do three things. First, we extend the work of Mensch and Rasolofosaon (1997) by seeking perturbation-theory solutions of the Christoffel equation in the WCS that include qP- and qS-wave polarization expressions in addition to phase velocities. We compare and contrast our polarization expressions with those discussed by others. Second, we develop first-order qP- and qS-wave group-velocity expressions that provide the direction of propagation of seismic energy in weak but arbitrarily anisotropic media. Despite their physical significance, qP- and qS-wave group-velocity expressions for waves propagating in weakly anisotropic elastic media have not been studied in sufficient generality. Our first-order group-velocity expressions, which are also developed with respect to the WCS, complement the suite of wave-attribute expressions already discussed in the literature. Finally, we use orthorhombic symmetry to illustrate how our general expressions can be used to derive explicit wave-attribute expressions for media with any given symmetry. Numerically, we examine the domain of applicability of the approximate polarization and group-velocity expressions and address problems associated with qS-wave expressions near the singularity directions.

CHRISTOFFEL EQUATION AND COORDINATE SYSTEM CONSIDERATIONS

It is well known (Auld, 1973; Carcione, 2001) that the Christoffel equation may be written as an eigenvector system of equations:

$$H_{ij}u_j = \lambda u_i \ (i = 1, 2, 3; \text{ sum over } j \text{ from 1 to 3}). \quad (1)$$

Here and throughout this paper we adopt the usual summation convention for repeated indices. Roman subscripts denote components of vectors or tensors relative to some Cartesian coordinate system. The eigenvector $\mathbf{u}$ determines the wave polarization, and the corresponding eigenvalue λ determines the wave phase velocity v according to

$$v = \sqrt{\frac{\lambda}{\rho}}, \quad (2)$$

where ρ is the mass density of the medium. The symmetric 3×3 matrix $\mathbf{H}$, called the Christoffel matrix (Auld, 1973), has components related to the components of the elastic (stiffness) tensor C_{ijkl} of the medium and to the direction of the wave vector $\mathbf{k}$ of the wave. Explicitly,

$$H_{ij} = C_{irsj}e_r^{(3)}e_s^{(3)}, \quad (3)$$

where $\mathbf{e}^{(3)}$ is a unit vector in the direction of $\mathbf{k}$. The reason for the superscript 3 is explained below. Components of the stiffness tensor C_{ijkl} in a given coordinate system are referred to as stiffness components for that coordinate system.

Our goal is to obtain first-order solutions to the eigenvalue problem posed by the Christoffel equation for weak but arbitrarily anisotropic media. Based on important structural simplifications of the Christoffel equation in the WCS, we will seek a perturbation theory solution of the equation directly in the WCS. Figure 1 shows the orientation of the WCS relative to the acquisition coordinate system. The acquisition coordinate system, otherwise known as the field coordinates, is the system with respect to which data are acquired and physical measurements are made. In a laboratory setting, the acquisition coordinate system is the same as the laboratory coordinate system. The acquisition coordinate system, with its z-axis oriented perpendicular to the earth's surface and increasing downward, is represented by $\{x, y, z\}$. The basis vectors for this coordinate system are the unit vectors $\mathbf{x}$, $\mathbf{y}$, and $\mathbf{z}$.

In Figure 1 the WCS is represented by the primed system $\{x',y',z'\}$, with the z'-axis oriented in the direction of the wave-vector $\mathbf{k}$ and the y'-axis oriented horizontally. For the unit basis vectors in the WCS, we use the superscript notation $\mathbf{e}^{(1)}$, $\mathbf{e}^{(2)}$, and $\mathbf{e}^{(3)}$ (rather than the notation $\mathbf{x}'$, $\mathbf{y}'$, and $\mathbf{z}'$) to facilitate writing and manipulating certain tensor expressions associated with the WCS.

The spherical coordinates θ and ϕ shown in Figure 1 denote the polar and azimuthal angles of $\mathbf{k}$ relative to the acquisition coordinate system. The unit basis vectors of the two coordinate systems

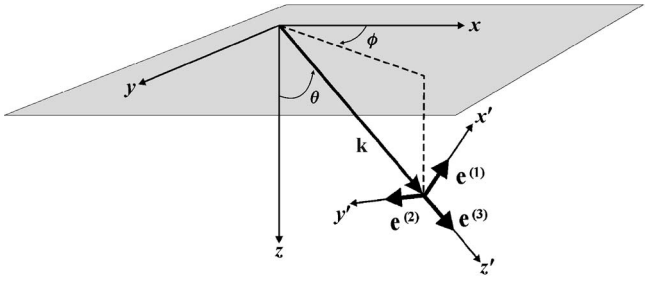

Figure 1. Orientations of the acquisition coordinate system $\{x, y, z\}$ and the WCS $\{x', y', z'\}$. The two systems are connected through the spherical coordinates (θ, ϕ). The z-axis of the acquisition system is in the vertical direction, and the z'-axis of the WCS is in the wave-vector direction $\mathbf{k} = \mathbf{e}^{(3)}$.

are related via these angles according to the well-known relations (Symon, 1971)

$$\mathbf{e}^{(1)} = \cos\theta\cos\phi\mathbf{x} + \cos\theta\sin\phi\mathbf{y} - \sin\theta\mathbf{z},$$

$$\mathbf{e}^{(2)} = -\sin\phi\mathbf{x} + \cos\phi\mathbf{y},$$

$$\mathbf{e}^{(3)} = \sin\theta\cos\phi\mathbf{x} + \sin\theta\sin\phi\mathbf{y} + \cos\theta\mathbf{z}. \quad (4)$$

The components of any vector **v** relative to the WCS are denoted with primes as v_1', v_2', and v_3'. Relative to the acquisition coordinates, the components of the same vector are denoted without primes as $\mathbf{v}_1$, $\mathbf{v}_2$, and $\mathbf{v}_3$. The components of **v** in the WCS may be expressed in terms of its components in the acquisition coordinates according to

$$v' = \mathbf{v}\cdot\mathbf{e}^{(a)} = \mathbf{v}_i e_i^{(a)} \quad (a = 1,2,3), \quad (5)$$

where $e_i^{(a)}$ with $i = 1, 2, 3$ are the acquisition-system components of the unit vector $\mathbf{e}^{(a)}$. These components may be read directly from equation 4, for example, $e_2^{(1)} = \cos\theta\sin\phi$. Likewise, for tensors such as H_{ij} and C_{ijkl}, we have

$$H'_{ab} = H_{ij}e_i^{(a)}e_j^{(b)} \quad (6)$$

and

$$C'_{abcd} = C_{ijkl}e_i^{(a)}e_j^{(b)}e_k^{(c)}e_l^{(d)}. \quad (7)$$

The relationship in equation 7 shows how the components of the fourth-rank stiffness tensor in the WCS can be expressed in terms of its components with respect to the acquisition coordinates. A more tractable method of relating stiffness components in the two coordinate systems is offered by the Bond matrix method (Auld, 1973). The advantage of the Bond transformation matrix is that it is applied directly to the Voigt indices of the tensor. (Voigt notation abbreviates the indices by replacing the first and last pair of indices of C_{ijkl} by single integers according to $11 \rightarrow 1$, $22 \rightarrow 2$, $33 \rightarrow 3$, 23 or $32 \rightarrow 4$, 13 or $31 \rightarrow 5$, 12 or $21 \rightarrow 6$). The stiffness components are then denoted C_{ij} in the acquisition coordinate system and C'_{ij} in the WCS, with i and j running from 1 to 6.) Equation 7 may then be replaced by the highly efficient transformation equation

$$C'_{rs} = M_{ri}M_{sj}C_{ij}, \quad (8)$$

where the explicit form of the 6×6 Bond matrix **M** is given in Appendix A. Through equation 8 each C'_{rs} in the WCS may be interpreted as an abbreviation for a specific linear combination of C_{ij} in the acquisition coordinate system with coefficients that are functions of the propagation angles θ and ϕ. This means that an expression (such as a velocity or polarization formula) written in terms of WCS stiffness components may be interpreted via equation 8 as an abbreviated form of the expression in the acquisition coordinates.

CHRISTOFFEL EQUATION IN THE WAVE-VECTOR COORDINATE SYSTEM

In this section we write the Christoffel equation explicitly in the WCS and cast it in a form conducive to the application of first-order perturbation theory. We begin by using equations 3, 6, and 7 to obtain

$$H'_{ij} = H_{ab}e_a^{(i)}e_b^{(j)} = C_{arsb}e_r^{(3)}e_s^{(3)}e_a^{(i)}e_b^{(j)} = C'_{i33j}. \quad (9)$$

This shows the important fact that the components of the Christoffel matrix in the WCS are certain stiffness components in the WCS. In Voigt notation, the identity in equation 9 may be written concisely as

$$H'_{ij} = C'_{(6-i)(6-j)}, \quad (10)$$

where i and j range from 1 to 3. Equation 10 holds only in the WCS (and in coordinate systems obtained from the WCS by rotation about $\mathbf{e}^{(3)}$).

Since the Christoffel equation 1 is a tensor equation, it must have the same form in the WCS. Thus,

$$H'_{ij}u'_j = \lambda u'_i. \quad (11)$$

Now, using equation 10 to write out equation 11 explicitly as

$$\begin{bmatrix} C'_{55} & C'_{45} & C'_{35} \\ C'_{45} & C'_{44} & C'_{34} \\ C'_{35} & C'_{34} & C'_{33} \end{bmatrix}\begin{bmatrix} u'_1 \\ u'_2 \\ u'_3 \end{bmatrix} = \lambda\begin{bmatrix} u'_1 \\ u'_2 \\ u'_3 \end{bmatrix}, \quad (12)$$

we arrive at the Christoffel equation in the WCS. Mensch and Rasolofosaon (1997) obtain this representation for the Christoffel matrix through two coordinate rotations.

Equation 12 displays the six conspicuous stiffness components — C'_{33}, C'_{44}, C'_{55}, C'_{34}, C'_{35}, and C'_{45} — that make up the elements of the Christoffel matrix $\mathbf{H}'$ in the WCS. Evidently, for a given wave-propagation direction, the exact solutions of the Christoffel equation for media with arbitrary anisotropy are expressible in terms of these six WCS stiffness components. As stated earlier, through equation 8 the WCS solutions of the Christoffel equation also exhibit the explicit form of the solutions with respect to the acquisition coordinates. Thus, the full complement of the stiffness components with respect to the acquisition coordinates, which is generally 21, would be revealed. The economy in the number of independent stiffness components entering the WCS Christoffel matrix substantially simplifies the bookkeeping in the analytic treatment of the problem as well as the presentation of the results. It is also important to recognize that the solutions in the WCS have no less physical significance than in the acquisition coordinate system. The physical meaning of C'_{ij}, the elements of the Christoffel matrix in the WCS, is clear: They are the stiffness components of the medium as one would measure by squeezing and shearing the medium in directions defined by the axes of the WCS.

For isotropic media, the Christoffel matrix in the WCS is simplified even further: It is strictly diagonal. This follows from the fact that for isotropic media, irrespective of the choice of the coordinate system, the stiffness components C_{ijkl} with an odd number of repeated indices must vanish (Auld, 1973).

PERTURBATION-THEORY SOLUTION OF THE CHRISTOFFEL EQUATION

The economy in the number of independent stiffness components in the WCS Christoffel matrix $\mathbf{H}'$ for general anisotropy and the strict diagonal form of $\mathbf{H}'$ for isotropy make the WCS a natural coordinate system for the application of perturbation theory to the weak anisotropy problem. Perturbation theory has been discussed extensively in the quantum mechanical literature (Landau and Lifschitz, 1977). It provides a method of finding approximate eigenvalues and eigenvectors of a symmetric matrix $\mathbf{H}$ if we know the eigenvalues and eigenvectors of another symmetric matrix $\mathbf{H}^0$ that approximates $\mathbf{H}$. We now use the methodology of perturbation theory to obtain approximate eigenvalues and eigenvectors for $\mathbf{H}'$ corresponding to weak anisotropy.

For weak anisotropy we can approximate $\mathbf{H}'$, the Christoffel matrix of the weakly anisotropic medium in the WCS by the Christoffel matrix $\mathbf{H}^{0\prime}$ of a suitably chosen isotropic medium. Because $\mathbf{H}^{0\prime}$ is also represented with respect to the WCS, it is diagonal and may be written

$$\mathbf{H}^{0\prime} = \begin{bmatrix} C_{44}^{0\prime} & 0 & 0 \\ 0 & C_{44}^{0\prime} & 0 \\ 0 & 0 & C_{33}^{0\prime} \end{bmatrix}, \tag{13}$$

where the elements $C_{33}^{0\prime}$ and $C_{44}^{0\prime}$ determine the elastic properties of the isotropic medium (Auld, 1973).

The values of $C_{33}^{0\prime}$ and $C_{44}^{0\prime}$ appearing in equation 13 may be chosen in any manner that makes $\mathbf{H}^{0\prime}$ a good approximation to $\mathbf{H}'$ for the weakly anisotropic medium of interest. In this paper, we take $C_{33}^{0\prime}$ and $C_{44}^{0\prime}$ to be the values of C_{33}' and C_{44}' of $\mathbf{H}'$ for the particular choice of the WCS corresponding to vertical wave propagation. For vertically propagating waves, except for a possible rotation about the vertical axis, the WCS coincides with the acquisition coordinate system. Thus, our choice amounts to setting $C_{33}^{0\prime} = C_{33}$, where C_{33} is the stiffness component as measured in the acquisition coordinate system for the weakly anisotropic medium. As for $C_{44}^{0\prime}$, any of the choices $C_{44}^{0\prime} = C_{44}$, $C_{44}^{0\prime} = C_{55}$, or $C_{44}^{0\prime} = (C_{44} + C_{55})/2$ would be suitable since $C_{44} \approx C_{55}$ for any weakly anisotropic medium. In this paper we choose $C_{44}^{0\prime} = C_{44}$. Numerical estimates for C_{33} and C_{44} can be obtained from the near-vertical propagating qP- and qS-wave phase velocities (Mensch and Rasolofosaon, 1997).

Since equation 13 with $C_{33}^{0\prime} = C_{33}$ and $C_{44}^{0\prime} = C_{44}$ approximates $\mathbf{H}'$ for weak anisotropy, we conclude that $\mathbf{H}'$ is approximately diagonal and its off-diagonal elements C_{34}', C_{35}', and C_{45}' are small compared to C_{33} and C_{44}. Likewise, the differences $C_{33}' - C_{33}$, $C_{44}' - C_{44}$, and $C_{55}' - C_{44}$ are small compared to C_{33} and C_{44}. We adopt the conventional terminology of perturbation theory when using the descriptions zero order, first order, etc. (Landau and Lifschitz, 1977). Thus, we say that C_{33} is the zero-order approximation to C_{33}' and that C_{44} is the zero-order approximation for both C_{44}' and C_{55}'. Expressions such as C_{34}'/C_{33}, $(C_{33}' - C_{33})/C_{33}$, and $(C_{55}' - C_{44})/C_{44}$ are small, first-order quantities. The product of two first-order quantities is a second-order quantity, and so forth. These order-of-magnitude relationships between the C_{ij}' of the WCS and the components C_{33} and C_{44} of the acquisition coordinate system facilitate the algebraic manipulations involved in the perturbation-theory solution of the weak anisotropy problem discussed next.

qP-wave phase velocities and polarization vectors for general weak anisotropy

To obtain first-order solutions to equation 12 corresponding to (quasi-) longitudinal waves (qP-waves), we note that in a weakly anisotropic medium, the longitudinal component u_3' of the polarization will be much larger than either transverse component u_1' or u_2' (u_1' and u_2' would be zero in an isotropic medium). Thus, for qP-waves we may consider u_1' and u_2' as small, first-order quantities compared to u_3'.

Writing equation 12 to the first order for a qP-wave yields

$$\begin{cases} C_{55}'u_1' + C_{35}'u_3' = \lambda u_1' \\ C_{44}'u_2' + C_{34}'u_3' = \lambda u_2' \\ C_{33}'u_3' = \lambda u_3' \end{cases}. \tag{14}$$

These lead directly to

$$\lambda = C_{33}' \tag{15}$$

and

$$u_1' = \frac{C_{35}'}{C_{33}' - C_{55}'}u_3', \quad u_2' = \frac{C_{34}'}{C_{33}' - C_{44}'}u_3'. \tag{16}$$

Here, $\mathbf{u}$ is a first-order unit vector if we take $u_3' = 1$. The denominators in equation 16 may be replaced by their zero-order approximations, and the overall expressions will still be accurate to first order. Thus, the first-order qP-wave unit polarization vector is

$$\mathbf{u}_{qP} = \frac{C_{35}'}{C_{33} - C_{44}}\mathbf{e}^{(1)} + \frac{C_{34}'}{C_{33} - C_{44}}\mathbf{e}^{(2)} + \mathbf{e}^{(3)}. \tag{17}$$

This expression agrees with the qP-wave polarization formula discussed by Pšenčík and Gajewski (1998).

The qP-wave phase velocity is obtained by substituting equation 15 into equation 2:

$$v_{qP} = \sqrt{\frac{C_{33}'}{\rho}}. \tag{18}$$

Equation 18 gives a compact, approximate expression for the qP-wave phase velocity in any weakly anisotropic medium. Equation 18 may be linearized to first-order accuracy as follows:

$$\begin{aligned} v_{qP} &= \sqrt{\frac{C_{33}'}{\rho}} \\ &= \sqrt{\frac{C_{33}}{\rho}\left(1 + \frac{C_{33}' - C_{33}}{C_{33}}\right)} \\ &= v_P^0\left(1 + \frac{C_{33}' - C_{33}}{2C_{33}}\right), \end{aligned} \tag{18a}$$

where $v_P^0 = \sqrt{C_{33}/\rho}$. Equation 18a displays the qP-wave phase velocity as a zero-order approximation v_P^0 plus a first-order correction. We note that for vertical propagation in the acquisition coor-

dinate system, $C'_{33} = C_{33}$. Therefore, equation 18a shows that v_P^0 is equal to the vertical qP-wave phase velocity to first-order accuracy.

The qP-wave polarization and phase-velocity expressions (equations 17 and 18), along with those for the qS-waves to be discussed next and the qP- and qS-wave group-velocity expressions to be discussed later, demonstrate the compactness and physical interpretability of solutions to the Christoffel equation in the WCS. We display these wave attributes in terms of the WCS stiffness components C'_{ij} and the WCS basis vectors $\mathbf{e}^{(i)}$. Each C'_{ij} appearing in our formulas has the physical meaning of being a stiffness component of the medium as measured directly in the WCS. For surface seismic exploration, these wave attributes need to be written with respect to the acquisition coordinate system. For this purpose, through equation 8, each C'_{ij} appearing in our expressions can be expanded in terms of C_{kl}, the stiffness components of the medium with respect to the acquisition coordinate system. Equation 4 provides the rule for transforming the WCS basis vectors $\mathbf{e}^{(i)}$ to the acquisition system $\{\hat{x},\hat{y},\hat{z}\}$.

As an illustration, consider the qP-wave phase-velocity expression 18a. It can be written with respect to the acquisition coordinate system by using equation 8 to express C'_{33} as

$$C'_{33} = M_{3i}M_{3j}C_{ij}, \tag{19}$$

with $\mathbf{M}$ as given in Appendix A. Equation 18a then becomes identical to equation 8 of Gajewski and Pšenčík (1996). As expected, when written out explicitly with respect to the acquisition coordinate system, v_{qP} becomes fairly lengthy and complex.

qS-wave phase velocities and polarization vectors for general weak anisotropy

For qS-waves, u'_3 is a small, first-order quantity compared with u'_1 or u'_2. Keeping only terms up to the first order in equation 12 yields

$$\begin{cases} C'_{55}u'_1 + C'_{45}u'_2 = \lambda u'_1 \\ C'_{45}u'_1 + C'_{44}u'_2 = \lambda u'_2 \\ C'_{35}u'_1 + C'_{34}u'_2 + C'_{33}u'_3 = \lambda u'_3 \ . \end{cases} \tag{20}$$

The first two equations have nontrivial solutions only if

$$\begin{vmatrix} C'_{55} - \lambda & C'_{45} \\ C'_{45} & C'_{44} - \lambda \end{vmatrix} = 0. \tag{21}$$

Thus, as expected, we generally have two values for λ corresponding to two distinct qS-wave modes:

$$\lambda_\pm = \frac{1}{2}[C'_{44} + C'_{55} \pm \sqrt{(C'_{44} - C'_{55})^2 + 4C'^2_{45}}]. \tag{22}$$

The plus sign corresponds to the faster qS-wave. Note that the two qS-wave phase velocities are equal to one another (degenerate) to the first-order only if $C'_{44} = C'_{55}$ and $C'_{45} = 0$. Equation 22 agrees with equation 34 of Mensch and Rasolofosaon (1997). A density-normalized version of equation 22 is also developed by Jech and Pšenčík (1989) and Farra and Pšenčík (2003).

For convenience in writing the results for the qS-wave polarization directions, we introduce an angle α, lying between $-\pi/2$ and $\pi/2$, defined by

$$\alpha = \frac{1}{2}\arctan[C'_{55} - C'_{44}, 2C'_{45}], \tag{23}$$

where $\arctan[x,y]$ is defined to be the angle θ lying between $-\pi$ and π such that $x = r\cos\theta$, $y = r\sin\theta$, and $r = \sqrt{x^2 + y^2}$. (Thus, the range of our arctangent function is not restricted to principal values.)

Substituting equation 22 into the first equation of equation 20 yields

$$\left(\frac{u'_2}{u'_1}\right)_+ = \tan\alpha \text{ and } \left(\frac{u'_2}{u'_1}\right)_- = -\cot\alpha. \tag{24}$$

The plus and minus subscripts correspond to the faster and slower (quasi-) qS-waves, respectively. Thus, for the faster wave we take $u'_1 = \cos\alpha$ and $u'_2 = \sin\alpha$, while for the slower wave we take $u'_1 = -\sin\alpha$ and $u'_2 = \cos\alpha$. In the language of degenerate perturbation theory (Landau and Lifshitz, 1977), these results give us the zero-order approximation for the unit polarization vectors corresponding to the faster and slower qS-waves:

$$\mathbf{u}^+_{S0} = \cos\alpha\mathbf{e}^{(1)} + \sin\alpha\mathbf{e}^{(2)}, \tag{25}$$

$$\mathbf{u}^-_{S0} = -\sin\alpha\mathbf{e}^{(1)} + \cos\alpha\mathbf{e}^{(2)}. \tag{25a}$$

Proceeding to the first-order approximations, after some algebra, we find that we can express the qS-wave polarization vectors in the following form:

$$\mathbf{u}^+_{qS} = \cos(\alpha + \Delta\alpha)\mathbf{e}^{(1)} + \sin(\alpha + \Delta\alpha)\mathbf{e}^{(2)} + \left(\frac{C'_{35}\cos\alpha + C'_{34}\sin\alpha}{C_{44} - C_{33}}\right)\mathbf{e}^{(3)}, \tag{26}$$

$$\mathbf{u}^-_{qS} = -\sin(\alpha + \Delta\alpha)\mathbf{e}^{(1)} + \cos(\alpha + \Delta\alpha)\mathbf{e}^{(2)} + \left(\frac{C'_{34}\cos\alpha - C'_{35}\sin\alpha}{C_{44} - C_{33}}\right)\mathbf{e}^{(3)}, \tag{26a}$$

where α is given by equation 23 and

$$\Delta\alpha = \frac{1}{C_{44} - C_{33}}\left[\frac{C'_{45}(C'^2_{34} - C'^2_{35}) + C'_{34}C'_{35}(C'_{55} - C'_{44})}{(C'_{55} - C'_{44})^2 + 4C'^2_{45}}\right]. \tag{27}$$

There is an important restriction on the validity of our expressions for the qS-wave polarization vectors. Generally, in an anisotropic medium there exist certain isolated directions of wave propagation for which the qS-wave polarization angle α is indeterminate because of degeneracy of the two qS-wave phase velocities. As previously noted, these degenerate directions occur in our first-

order treatment whenever both $C'_{55} = C'_{44}$ and $C'_{45} = 0$. Equations 23 and 27 thus show that both α and $\Delta\alpha$ are undefined at the degenerate directions. In the immediate neighborhood of a degenerate direction, α and $\Delta\alpha$ tend to be unstable with regard to small variations in the elastic properties of the medium. Therefore, equations 23 and 27 are not reliable in the vicinity of *S*-wave degeneracy. Moreover, inspection of equation 27 shows that $\Delta\alpha$ actually diverges when approaching a degenerate direction because the denominator in equation 27 approaches zero faster than the numerator as both $(C'_{55} - C'_{44})$ and C'_{45} approach zero. Thus, in the neighboring directions of degeneracy, $\Delta\alpha$ is not a valid first-order correction to the zero-order angle α. In fact, near degenerate directions, the first-order approximation $\alpha + \Delta\alpha$ can be less accurate than the zero-order approximation α. This behavior is illustrated later with numerical evaluations.

Jech and Pšenčík (1989) use perturbation theory to derive expressions for both zero-order and first-order approximations for qS-wave polarizations in an arbitrary weakly anisotropic medium. Except for the zero-order expressions, our results are equivalent to theirs. Our zero-order qS-wave polarization expressions agree with formulas discussed by Thomson et al. (1992) and Farra and Pšenčík (2003).

The introduction of the qS-wave polarization angle α, together with the use of the WCS basis vectors $(\mathbf{e}^{(1)}, \mathbf{e}^{(2)}, \mathbf{e}^{(3)})$, allows us to express our qS-wave polarization expressions in a form that clearly displays the geometry of the polarization directions. As equations 25 and 25a show, to the lowest (zero) order of approximation, the qS-wave polarization vectors $\mathbf{u}^{+}_{S0}$ and $\mathbf{u}^{-}_{S0}$ are obtained by rotating $\mathbf{e}^{(1)}$ and $\mathbf{e}^{(2)}$ about $\mathbf{e}^{(3)}$ by the angle α. Equations 26 and 26a explicitly give the qS-wave polarizations relative to the WCS in terms of the polarization angles defined in equations 23 and 27. They show that the effect of the first-order correction is to introduce a small component along the wave vector $\mathbf{e}^{(3)}$ and to add a small angular correction $\Delta\alpha$ to α. Transformation to the acquisition coordinate system may be accomplished using equations 4 and 8.

The faster and slower qS-wave phase velocities are found by substituting the qS-wave eigenvalues of equation 22 into equation 2. After performing manipulations similar to those indicated in equation 18a, we obtain

$$v^{\pm}_{qS} = v^{0}_{S}\left[1 + \left(\frac{C'_{55} + C'_{44} - 2C_{44} \pm \sqrt{(C'_{55} - C'_{44})^2 + 4{C'_{45}}^2}}{4C_{44}}\right)\right], \tag{28}$$

where $v^{0}_{S} = \sqrt{C_{44}/\rho}$. Here, v^{+}_{qS} is associated with the plus sign in front of the square root in equation 28 and denotes the phase velocity for the faster qS-wave. Similarly, v^{-}_{qS} corresponds to the slower qS-wave. Equation 28 agrees with Jech and Pšenčík (1989) and Mensch and Rasolofosaon (1997).

GROUP VELOCITIES IN GENERAL WEAKLY ANISOTROPIC MEDIA

Phase velocity characterizes the speed of propagation of a fixed value of phase of an infinitely extended plane (harmonic) wave. In practice, we do not deal with an ideal plane wave, but rather, with a wave that is limited in both spatial extent and duration. If the spatial and time limitations are not too extreme, then the wave may be considered to be a superposition of plane waves covering a rather narrow range of wave vectors centered around some average wave vector $\mathbf{k}_0$. The spread in wave vectors includes a variation in direction as well as magnitude. Although a specific value of phase of the wave group propagates essentially at the phase velocity corresponding to $\mathbf{k}_0$, the wave group as a whole and the energy carried by the wave propagate at a group velocity (ray velocity) that generally differs from the phase velocity in both direction and magnitude. For a graphic demonstration of group velocity arising from the superposition of two plane waves of the same frequency but slightly different wave-vector directions, see Wolfe and Hauser (1995). Ohanian et al. (1997) investigate acoustic wavefronts and group velocities as superposition of plane harmonic waves in anisotropic geologic sediments.

Letting $\omega(\mathbf{k}) = kv(\mathbf{k})$ denote the angular frequency of the harmonic component with wave vector $\mathbf{k}$, the group velocity vector $\mathbf{w}$ may be expressed as

$$\mathbf{w} = \nabla_{\mathbf{k}}\omega(\mathbf{k}) = \left(\mathbf{e}^{(1)}\frac{\partial}{k\partial\theta} + \mathbf{e}^{(2)}\frac{\partial}{k\sin\theta\partial\phi} + \mathbf{e}^{(3)}\frac{\partial}{\partial k}\right)\omega(\mathbf{k}), \tag{29}$$

where the *k*-space gradient operator $\nabla_{\mathbf{k}}$ is written out explicitly in terms of spherical coordinates of the acquisition coordinate system. [For a formal discussion of group velocities, see Auld (1973) and Wolfe and Hauser (1995).] These derivatives in equation 29 are to be evaluated at the average wave vector $\mathbf{k}_0$. Since the basis vectors of the spherical coordinates of the acquisition system are identical to the basis vectors of the WCS, equation 29 conveniently expresses the group velocity relative to the WCS.

The phase-velocity expressions derived earlier show that in an anisotropic medium, the phase velocity $v(\mathbf{k})$ depends explicitly on the direction of $\mathbf{k}$. However, since dispersion is largely absent for the long wavelengths used in seismic exploration, $v(\mathbf{k})$ has negligible dependence on the magnitude of $\mathbf{k}$. Thus, we may write $\omega(\mathbf{k}) = kv(\theta,\phi)$ and reduce equation 29 to an expression relating the group velocity to derivatives of the phase velocity:

$$\mathbf{w} = \frac{\partial v(\theta,\phi)}{\partial\theta}\mathbf{e}^{(1)} + \frac{\partial v(\theta,\phi)}{\sin\theta\partial\phi}\mathbf{e}^{(2)} + v(\theta,\phi)\mathbf{e}^{(3)}. \tag{30}$$

Denoting the group-velocity vector by its components $\mathbf{w} = w'_1\mathbf{e}^{(1)} + w'_2\mathbf{e}^{(2)} + w'_3\mathbf{e}^{(3)}$, we have

$$w'_1 = \frac{\partial v}{\partial\theta}, \quad w'_2 = \frac{1}{\sin\theta}\frac{\partial v}{\partial\phi}, \quad w'_3 = v. \tag{31}$$

Inspection of equations 18a and 28 shows that the P- and S-wave phase velocities depend on θ and ϕ only via the WCS stiffness components $C'_{33}, C'_{44}, C'_{45}$, and C'_{55} (whose functional dependence on θ and ϕ is given by equation 8). Therefore, the P- and S-wave group velocities involve derivatives of these stiffness components with respect to θ and ϕ. These derivatives can be shown to be expressible as linear functions of other WCS stiffness components. As a result, we obtain the following vector expression for the first-order qP-wave group velocity:

$$\mathbf{w}_{qP} = 2v_P^0\left(\frac{C'_{35}}{C_{33}}\mathbf{e}^{(1)} + \frac{C'_{34}}{C_{33}}\mathbf{e}^{(2)}\right) + v_{qP}\mathbf{e}^{(3)}, \qquad (32)$$

where v_{qP} is given by equation 18a. Similarly, for the qS-wave group velocities, we find

$$\mathbf{w}^{\pm}_{qS} = w_1'^{\pm}\mathbf{e}^{(1)} + w_2'^{\pm}\mathbf{e}^{(2)} + v^{\pm}_{qS}\mathbf{e}^{(3)}, \qquad (33)$$

where $v^{\pm}_{qS}$ is given in equation 28 and

$$w_1'^{\pm} = \frac{v_S^0}{2C_{44}}[C'_{15} + C'_{46} - C'_{35} \pm (C'_{15} - C'_{46} - C'_{35})\cos 2\alpha \pm (C'_{14} + C'_{56} - C'_{34})\sin 2\alpha], \qquad (33a)$$

$$w_2'^{\pm} = \frac{v_S^0}{2C_{44}}[C'_{24} + C'_{56} - C'_{34} \pm (C'_{34} + C'_{56} - C'_{24})\cos 2\alpha \pm (C'_{25} + C'_{46} - C'_{35})\sin 2\alpha]. \qquad (33b)$$

The upper-lower sign ($\pm$) in the above expressions for $w_1'^{\pm}$ and $w_2'^{\pm}$ corresponds to taking the upper/lower sign ($\pm$) in equation 28, and α is the polarization angle defined by equation 23.

The appearance of the polarization angle α in the first-order qS-wave group-velocity expressions is interesting. As stated earlier, whenever the phase velocities of the two qS-waves coincide, α becomes indeterminate. Therefore, like the first-order qS-wave polarization expressions, the derived first-order qS-wave group velocities are unreliable near the directions of S-wave degeneracy. This behavior is illustrated later with numerical evaluations of the group-velocity expressions.

Inspection of expressions 32 and 33 shows that the deviations of the directions of the qP- and qS-wave group velocities from the direction of the wave vector are linear functions of C'_{34}, C'_{35}, C'_{14}, C'_{15}, C'_{24}, C'_{25}, C'_{46}, and C'_{56}. For weak anisotropy, the magnitude of these stiffness components is, at most, first-order compared with C_{33} and C_{44}. This implies that $|\mathbf{w}| = v$ up to and including first-order accuracy. However, we see explicitly that weak anisotropy generates first-order deviations in the qP- and qS-wave group-velocity directions from the wave-vector direction. Later we present numerical tests that quantitatively illustrate the influence of anisotropy on these deviations.

Byun and Corrigan (1990) discuss an iterative model-based ray-tracing scheme to invert the traveltimes from field VSP data for the VTI stiffness components. For the purposes of computing first-arrival traveltimes in VTI media used in Kirchhoff migration, Faria and Stoffa (1994) incorporate Thomsen's group-velocity expressions to calculate ray directions. Cheadle et al. (1991) use group-velocity measurements taken directly along the symmetry planes and in 45° propagation directions of a phenolic cube to compute the stiffness components of an orthorhombic specimen. Our group-velocity expressions can facilitate the extension of similar algorithms to media with arbitrary symmetry.

APPLICATION TO WEAK ORTHORHOMBIC SYMMETRY

To illustrate the use of our general results, we focus on media possessing orthorhombic symmetry, which has direct practical applications in exploration (Schoenberg and Helbig, 1997). Tsvankin (1997) shows that in the symmetry planes of an orthorhombic medium, solutions to the Christoffel equation reduce to equivalent VTI expressions. Pšenčík and Gajewski (1998) derive first-order phase velocity and polarization relations for qP-waves in weak orthorhombic media. Farra and Pšenčík (2003) investigate additional wave attributes in orthorhombic media. We rederive some of these results and additionally obtain useful approximate qS-wave polarization and group-velocity expressions.

Instead of dealing explicitly with individual stiffness components, Thomsen (1986) simplifies the weak VTI problem by introducing his parameters ε, δ, and γ. Several authors extend his work to include media with arbitrary symmetry [Sayers (1994), Pšenčík and Gajewski (1998), Mensch and Rasolofosaon (1997)]. We proceed along similar lines to define weak-anisotropy parameters for use in our wave-attribute expressions.

The stiffness tensor C_{ij}^{ortho} of the standard orthorhombic medium (with its axes of symmetry coincident with the acquisition coordinate axes) has nine independent components (Tsvankin, 1997), whereas the isotropic stiffness tensor C_{ij}^{iso} has only two: C_{33} and C_{44} (Thomsen, 1986). Since for weak anisotropy, the difference between C_{ij}^{ortho} and C_{ij}^{iso} is small, it is natural to define the weak-anisotropy parameters g_{ij} by considering some dimensionless scaled version of $(C_{ij}^{\text{ortho}} - C_{ij}^{\text{iso}})$. The degree of anisotropy for an orthorhombic medium may be characterized by the following seven weak anisotropy parameters:

$$g_{11} = \frac{C_{11} - C_{33}}{2C_{33}}, \quad g_{22} = \frac{C_{22} - C_{33}}{2C_{33}},$$

$$g_{55} = \frac{C_{55} - C_{44}}{2C_{44}}, \quad g_{66} = \frac{C_{66} - C_{44}}{2C_{44}},$$

$$g_{12} = \frac{C_{12} + 2C_{66} - C_{33}}{C_{33}}, \quad g_{13} = \frac{C_{13} + 2C_{55} - C_{33}}{C_{33}},$$

$$g_{23} = \frac{C_{23} + 2C_{44} - C_{33}}{C_{33}}. \qquad (34)$$

For weak anisotropy, all g_{ij} are small compared to one and reduce to zero for the isotropic case. These parameters are identical to those of Pšenčík and Gajewski (1998), except that we introduce two additional parameters, g_{55} and g_{66}.

First-order phase velocities for weak orthorhombic media

Working with equations 18a and 28, after expanding each of the stiffness components C'_{kl} appearing in these expressions in terms of the C_{ij} and using equation 34 to eliminate C_{ij} in favor of g_{ij}, we ob-

tain the following first-order qP- and qS-wave phase-velocity expressions for waves propagating in weakly orthorhombic media:

$$v_{qP} = v_P^0(1 + P(\theta,\phi)), \tag{35}$$

$$v_{qS}^{\pm} = v_S^0[1 + S(\theta,\phi) \pm \sqrt{M(\theta,\phi)^2 + N(\theta,\phi)^2}]. \tag{35a}$$

The explicit dependence of these phase-velocity expressions (as well as the polarization and group-velocity expressions discussed next) on the weak-anisotropy parameters g_{ij} and the propagation directions θ and ϕ can be seen through the full form of the abbreviations $P(\theta,\phi)$, $S(\theta,\phi)$, $M(\theta,\phi)$, etc., provided in Appendix B.

First-order polarization vectors for weak orthorhombic media

After transforming the general weak-anisotropy polarization expressions 17, 26, and 26a to the acquisition coordinates and expressing them in terms of the weak orthorhombic parameters, we obtain the following first-order unit polarization vectors for qP- and qS-waves in weak orthorhombic media (see Appendix B):

$$\mathbf{u}_{qP} = A(\theta,\phi)\mathbf{e}^{(1)} + B(\theta,\phi)\mathbf{e}^{(2)} + \mathbf{e}^{(3)}, \tag{36}$$

$$\mathbf{u}_{qS}^{+} = \cos\alpha\mathbf{e}^{(1)} + \sin\alpha\mathbf{e}^{(2)} - [A(\theta,\phi)\cos\alpha + B(\theta,\phi)\sin\alpha]\mathbf{e}^{(3)}, \tag{36a}$$

$$\mathbf{u}_{qS}^{-} = -\sin\alpha\mathbf{e}^{(1)} + \cos\alpha\mathbf{e}^{(2)} - [B(\theta,\phi)\cos\alpha - A(\theta,\phi)\sin\alpha]\mathbf{e}^{(3)}. \tag{36b}$$

The polarization angle α, via the general expression 23, is

$$\alpha = \frac{1}{2}\arctan[M(\theta,\phi),N(\theta,\phi)] \text{ and } -\frac{\pi}{2} < \alpha < \frac{\pi}{2}. \tag{37}$$

For propagation in the symmetry planes of the orthorhombic medium, these expressions simplify. For example, using the explicit forms of $M(\theta,\phi)$ and $N(\theta,\phi)$ given in Appendix B, we can show that for each symmetry plane of the orthorhombic medium, equation 37 yields $\alpha = 0$ or $\pi/2$. This result is consistent with the polarization angle for a VTI system and provides an example of a general property discussed by Tsvankin (1997).

Inspection of equation 27 shows that the first-order correction to the polarization angle ($\Delta\alpha$) can become very complicated when it is written in terms of the stiffness components of the acquisition coordinate system. Numerical results of the next section provide insight into the accuracy of the zero-order and first-order expressions for the qS-wave polarization angles. There we show that the zero-order approximation for the polarization angle as given in equation 37 provides sufficient accuracy without including the first-order correction $\Delta\alpha$ for a wide range of propagation directions in a weak orthorhombic medium. For this reason, we set $\Delta\alpha = 0$ in the qS-wave polarization vector expressions 36a and 36b to keep them simple in form and without a significant loss in accuracy. To make these expressions truly accurate to first order, α should be replaced by $\alpha + \Delta\alpha$ in the coefficients of $\mathbf{e}^{(1)}$ and $\mathbf{e}^{(2)}$, as in equations 26 and 26a.

Equations 35 and 36 for the qP-wave phase velocity and polarization vector agree with formulas discussed by Pšenčík and Gajewski (1998). For additional discussions on qS-wave phase velocities, see Mensch and Rasolofosaon (1997).

First-order group velocities for weak orthorhombic media

From the general weak-anisotropy group-velocity expressions 32 and 33, we obtain the corresponding group-velocity formulas valid for weak orthorhombic media. With reference to the abbreviations in Appendix B, these group velocities can be written in the following convenient forms:

$$\mathbf{w}_{qP} = 2\left(1 - \frac{C_{44}}{C_{33}}\right)v_P^0[A(\theta,\phi)\mathbf{e}^{(1)} + B(\theta,\phi)\mathbf{e}^{(2)}] + v_{qP}\mathbf{e}^{(3)}, \tag{38}$$

$$\mathbf{w}_{qS}^{\pm} = w_1'^{\pm}\mathbf{e}^{(1)} + w_2'^{\pm}\mathbf{e}^{(2)} + v_{qS}^{\pm}\mathbf{e}^{(3)}, \tag{38a}$$

where

$$w_1'^{\pm} = F_1(\theta,\phi) \pm [G_1(\theta,\phi)\cos 2\alpha + H_1(\theta,\phi)\sin 2\alpha], \tag{38b}$$

$$w_2'^{\pm} = F_2(\theta,\phi) \pm [G_2(\theta,\phi)\cos 2\alpha + H_2(\theta,\phi)\sin 2\alpha]. \tag{38c}$$

The terms v_{qP} and $v_{qS}^{\pm}$ associated with the $\mathbf{e}^{(3)}$ components of group velocity expressions 38 and 38a denote the qP- and qS-wave phase velocities defined in equations 35 and 35a. An examination of the accuracy of equations 38 and 38a is provided in our later discussion on numerical evaluations of group velocities.

The approximate wave-attribute expressions for orthorhombic media discussed here can be shown to be exact for vertically propagating waves. Therefore, they are more accurate for waves propagating in directions that are closer to the vertical. Symmetry-plane projections of the derived approximate orthorhombic expressions reduce to equivalent VTI expressions.

NUMERICAL COMPARISON OF S-WAVE POLARIZATION EXPRESSIONS

In this section, we investigate the accuracy of the zero-order and first-order qS-wave polarization expressions 25, 25a, 26, and 26a by applying them to the orthorhombic model investigated by Schoenberg and Helbig (1997). The density-normalized elastic stiffness matrix of this model relative to the acquisition coordinate system is

$$(C_{ij}) = \begin{pmatrix} 9.00 & 3.60 & 2.25 & 0 & 0 & 0 \\ 3.60 & 9.84 & 2.40 & 0 & 0 & 0 \\ 2.25 & 2.40 & 5.94 & 0 & 0 & 0 \\ 0 & 0 & 0 & 2.00 & 0 & 0 \\ 0 & 0 & 0 & 0 & 1.60 & 0 \\ 0 & 0 & 0 & 0 & 0 & 2.18 \end{pmatrix}. \quad (39)$$

The anisotropy represented by this model is not weak. For example, C_{33} differs from C_{22} by about 65%, and the value of the associated weak anisotropy parameter g_{22} is about 0.33. The relatively strong anisotropy of this model provides a robust test of our polarization expressions. (For the same reason, we also use it next to evaluate group velocities.) Numerical studies of approximate formulas for qS-wave polarization directions for this model are given in Farra and Pšenčík (2003). Our purpose here is to evaluate and compare the accuracy of our WCS expressions for the zero-order and first-order qS-wave polarization angles and to illustrate their behavior near directions of S-wave degeneracy.

As predicted, the derived approximate polarization expressions are inaccurate for qS-waves propagating in directions close to singular directions. Figure 2 shows a contour map that displays the percent difference between the first-order faster and slower qS-wave phase velocities. Four dots mark the points where the faster and slower phase velocities are equal. These singular directions obtained from our first-order phase velocity expressions are at $(\theta, \phi) = (50.5°, 42.2°)$, $(20.1°, 0°)$, $(66.1°, 0°)$, and $(76.6°, 90°)$. The corresponding numerically computed exact directions are at $(\theta, \phi) = (46.5°, 44.9°)$, $(20.1°, 0°)$, $(59.8°, 0°)$, and $(72.5°, 90°)$.

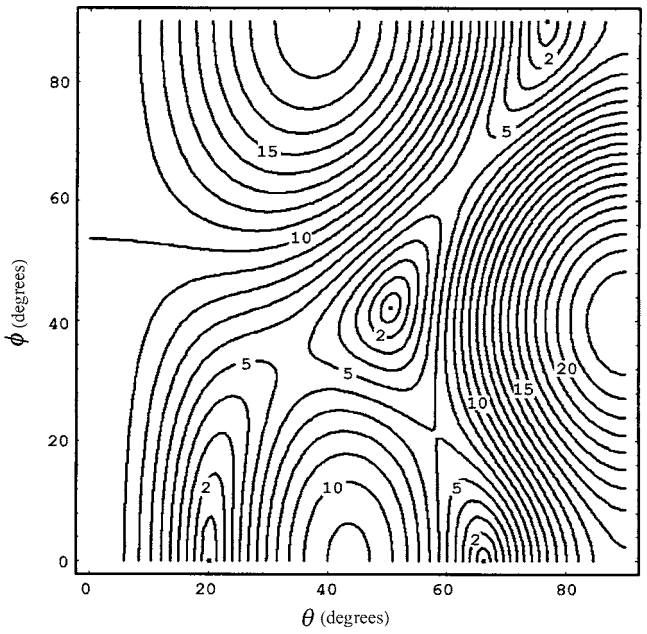

Figure 2. Contour map showing the percent difference between the faster and slower qS-wave phase velocities generated for the Schoenberg and Helbig orthorhombic model using the first-order approximation formulas. The percent difference is plotted as a function of the propagation direction angles θ and ϕ. Four dots mark the singular points where the faster and slower phase velocities are equal.

Figure 3 displays plots of the exact, first-order, and zero-order polarization angles of the faster qS-wave as a function of wave-vector direction. We plot the angle between $\mathbf{e}^{(1)}$ and the projection of the faster qS-wave polarization vector onto the $\mathbf{e}^{(1)} - \mathbf{e}^{(2)}$ plane. To zero-order approximation, this is α given in equation 23. To first-order approximation, the polarization angle is given by $\alpha + \Delta\alpha$, where $\Delta\alpha$ is given in equation 27. Exact polarization angles are obtained by a numerical solution of the Christoffel equation. The graphs cover one octant of space specified by the domain $0 < \theta < 90°$, $0 < \phi < 90°$. Each graph plots polarization angle versus θ for a fixed value of ϕ. Angular deviations between the approximate and exact polarization directions are interpreted as the error in the polarization angle.

Figure 3 shows that both zero-order and first-order approximations are quite accurate for θ, less than about 40° for all values of ϕ. For this restricted but rather large domain, the polarization error in the zero-order approximation remains less than 5°, while the error in the first-order approximation is less than 3°. In this domain,

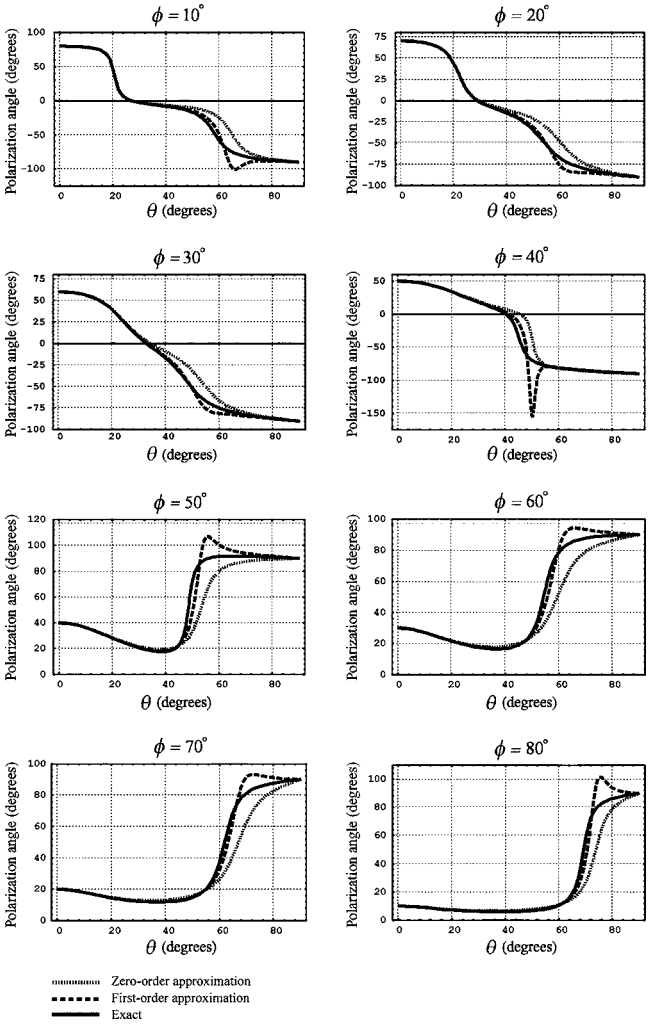

Figure 3. Comparison of the exact, first-order, and zero-order polarization angles for the faster qS-wave computed for the Schoenberg and Helbig model. The plots are generated as functions of θ for fixed values of the wave-vector azimuth angles ϕ ($\phi_0 = 10°$, $\phi_0 = 20°$, $\phi_0 = 30°$,…).

there is no significant advantage in including the first-order correction $\Delta\alpha$. In Figure 3, we also note that for the domain $40° < \theta < 60°$, the first-order correction provides noticeable improvement for most values of ϕ. However, near qS-wave degeneracy (ϕ near 40° and θ near 50°) the first-order approximation clearly breaks down and even gives poorer results than the zero-order approximation. As discussed earlier, this behavior is because of the divergence of the expression for $\Delta\alpha$ in equation 27 near the degenerate directions. We also notice that for the plots corresponding to $\phi = 10°$ and $\phi = 80°$, the first-order curves display inaccurate blips for θ near 65° and 75°, respectively. Again, this is because the qS-waves are nearly degenerate for these propagation directions.

In summary, the zero-order approximation for the qS-wave polarization is generally quite stable and accurate away from the singular directions. Although the first-order correction gives noticeable improvement in certain limited domains of propagation direction, it is more complicated in form than the zero-order approximation. For this particular model, the first-order approximation can give poorer results than the zero-order approximation near directions of qS-wave degeneracy. Very near the degenerate directions, neither the zero-order nor the first-order expressions can be expected to yield accurate results.

NUMERICAL EVALUATION OF GROUP-VELOCITY EXPRESSIONS

We now provide numerical evaluation of the accuracy of our first-order qP- and qS-wave group-velocity expressions. For this purpose, we again use the Schoenberg and Helbig (1997) orthorhombic model described by the elastic stiffness matrix (equation 39).

Since to the first order, in weak anisotropy, the magnitude of the group velocity is equal to the phase velocity, we consider only group-velocity directions. To describe the direction of the group-velocity vectors, we use polar and azimuthal angles (Θ, Φ) to specify deviations of the group velocity $\mathbf{w}$ from the wave vector $\mathbf{k}$. Figure 4 shows the orientation of $\mathbf{w}$ with respect to the WCS $(\mathbf{e}^{(1)}, \mathbf{e}^{(2)}, \mathbf{e}^{(3)})$ through the polar and azimuthal angles. Note that (Θ, Φ) are distinct from the polar angles (θ, ϕ), which specify the orientation of $\mathbf{k}$ with respect to the acquisition coordinate system (x, y, z) illustrated in Figure 1. The polar angle Θ denotes the angle between $\mathbf{k}$ and $\mathbf{w}$. This angle determines a cone on which the group velocity must lie. The azimuthal angle Φ locates the group velocity on the cone. It denotes the angle between $\mathbf{e}^{(1)}$ and the projection of $\mathbf{w}$ onto the $\mathbf{e}^{(1)} - \mathbf{e}^{(2)}$ plane. Recalling the notation used earlier to describe the group-velocity vector by its components, $\mathbf{w} = w_1'\mathbf{e}^{(1)} + w_2'\mathbf{e}^{(2)} + w_3'\mathbf{e}^{(3)}$, the polar and azimuthal group-velocity angular deviations from the direction of the wave vector are given by:

$$\Theta(\theta,\phi) = \tan^{-1}\left[\frac{\sqrt{(w_1')^2 + (w_2')^2}}{w_3'}\right],$$

$$\Phi(\theta,\phi) = \tan^{-1}\left[\frac{w_2'}{w_1'}\right]. \qquad (40)$$

For weak media, Θ is always small. However, Φ can be any angle.

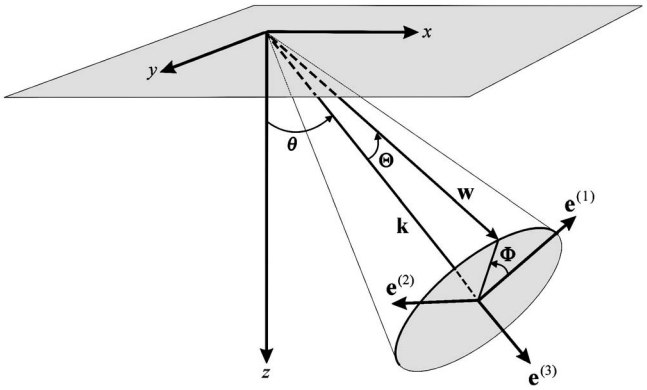

Figure 4. Illustration of the direction of group velocity $\mathbf{w}$ with respect to the WCS basis vectors $(\mathbf{e}^{(1)}, \mathbf{e}^{(2)}, \mathbf{e}^{(3)})$ through the polar and azimuthal angles (Θ, Φ). Equations 40 give (Θ, Φ) as functions of the wave-vector direction angles θ and ϕ, illustrated in Figure 1.

Figures 5–7 compare the first-order and exact qP- and qS-wave

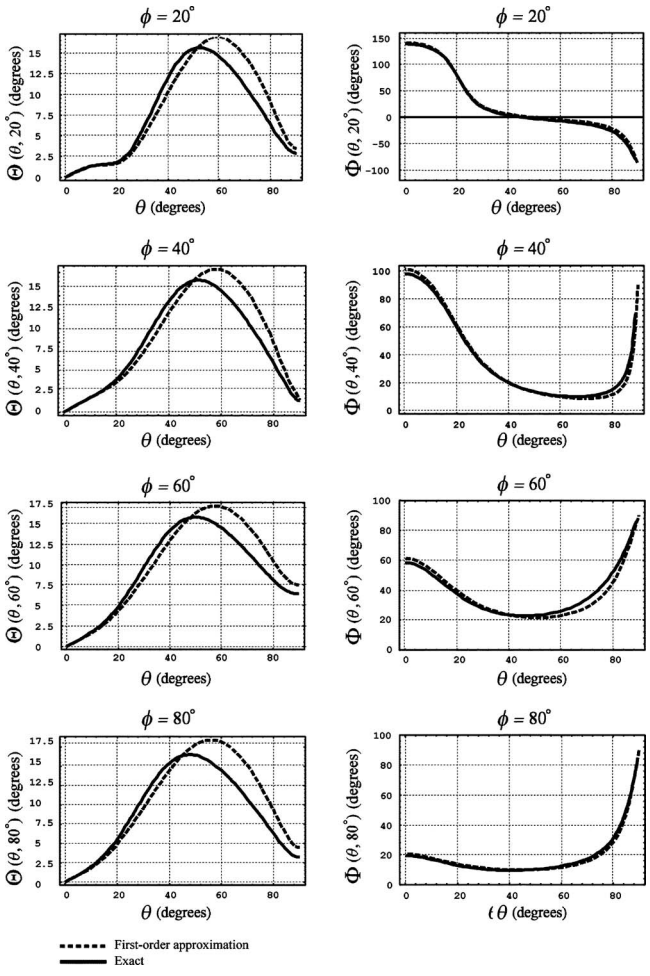

Figure 5. Comparison of the exact and first-order group-velocity directions for qP-waves for the Schoenberg and Helbig orthorhombic model. Shown are plots of the functions (left) $\Theta(\theta, \phi_0)$ and (right) $\Phi(\theta, \phi_0)$ versus θ for fixed values of ϕ ($\phi_0 = 20°$, $\phi_0 = 40°$, $\phi_0 = 60°$, and $\phi_0 = 80°$). The first-order qP-wave results are computed using equation 38.

group-velocity directions for the Schoenberg and Helbig model. Figure 5 corresponds to qP-waves, Figure 6 corresponds to slow qS-waves, and Figure 7 corresponds to fast qS-waves. For each mode, for fixed values of ϕ ($\phi_0 = 20°$, $\phi_0 = 40°$, $\phi_0 = 60°$, and $\phi_0 = 80°$), we use equation 40 to generate plots of $\Theta(\theta, \phi_0)$ and $\Phi(\theta, \phi_0)$ versus θ. We obtain the exact directions by numerical solution of the Christoffel equation. Although we display results for fixed values of ϕ (in 20° intervals), these plots illustrate the substance of our general conclusions, based on our investigation of the entire domain $0 < \theta < 90°, 0 < \phi < 90°$. The deviation between the first-order and the exact results is called the error in the first-order group-velocity direction.

Referring to Figure 5, we first consider the qP-wave group-velocity polar direction plots $\Theta(\theta, \phi_0)$ (left column). As the graphs for all ϕ values show, in the domain $0 < \theta < 50°$, the angular deviation of the group velocity from the wave vector can be as large as 16°. In the same domain, as can be confirmed by inspection, the first-order curves underestimate the exact curves by less than 3°. Beyond $\theta = 50°$ up to $\theta = 90°$, the first-order $\Theta(\theta, \phi_0)$ graphs closely follow the trend of the exact curves and overestimate them by less than 5°. Considering the qP-wave group-velocity azimuthal direction plots $\Phi(\theta, \phi_0)$ (right column), we note that for all propagation directions ($0 < \theta < 90°$) and for all ϕ_0 values, the errors in the first-order azimuthal angle remain less than 5°, even though the azimuthal angle itself undergoes large changes.

Figure 6 shows group-velocity direction plots for the slow qS-waves. Here, inspection of the polar direction graphs $\Theta(\theta, \phi_0)$ shows that the first-order approximation is quite accurate for θ less than 40° and for all ϕ values. For this near-vertical sector, the angular deviation of the group velocity from the wave-vector direction can be as large as 30°, while the error in the first-order results remains less than 2°. Within the same range of near-vertical propagation directions ($0 < \theta < 40°$), the errors in the slow qS-wave azimuthal direction graphs $\Phi(\theta, \phi_0)$ are hardly observable. For propagation directions away from the vertical ($40° < \theta < 90°$), the first-order polar and azimuthal direction graphs (for all ϕ values) closely follow the trends of the corresponding exact results. However, the first-order graphs for both $\Theta(\theta, \phi_0)$ and $\Phi(\theta, \phi_0)$ are shifted laterally with respect to the exact results, making the first-order results less reliable for $\theta > 40°$.

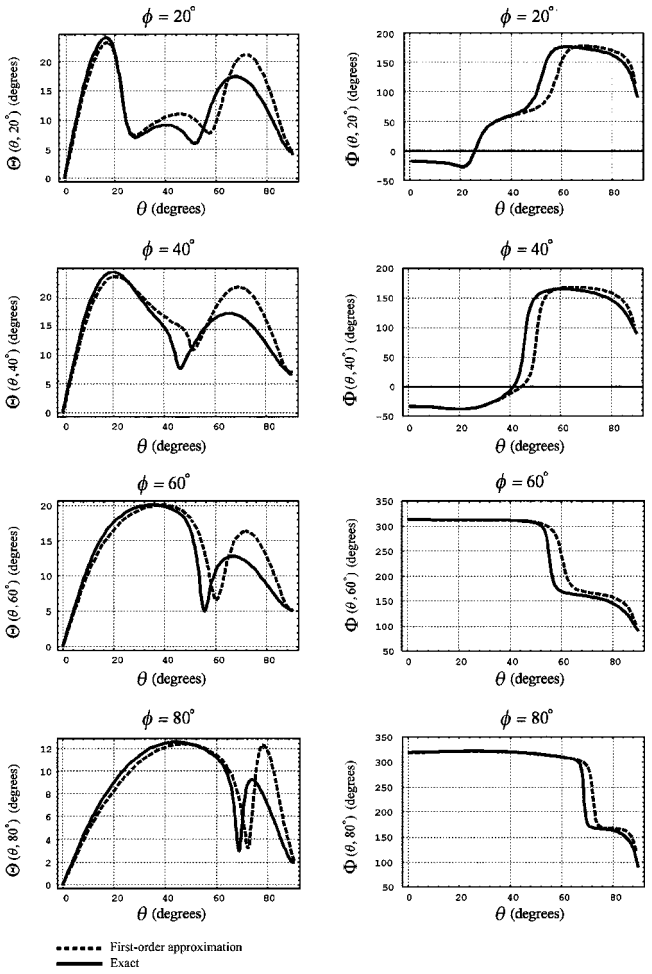

Figure 6. Comparison of the exact and first-order group-velocity directions for slow qS-waves for the Schoenberg and Helbig orthorhombic model. Shown are plots of the functions (left) $\Theta(\theta, \phi_0)$ and (right) $\Phi(\theta, \phi_0)$ versus θ for fixed values of ϕ ($\phi_0 = 20°$, $\phi_0 = 40°$, $\phi_0 = 60°$, and $\phi_0 = 80°$). The first-order results are obtained from equation 38a.

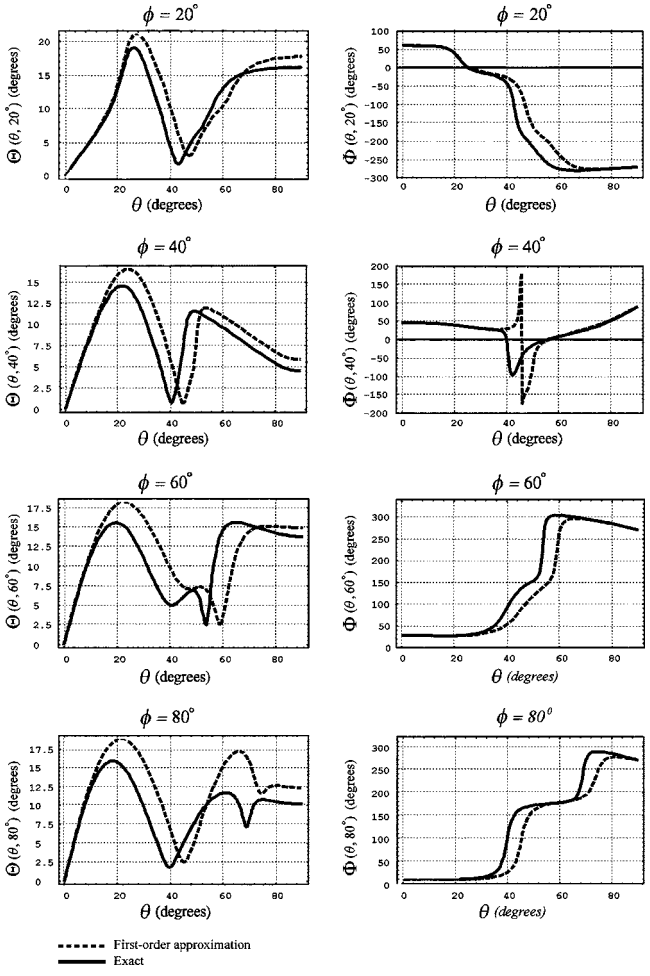

Figure 7. Comparison of the exact and first-order group-velocity directions for fast qS-waves for the Schoenberg and Helbig orthorhombic model. Shown are plots of the functions (left) $\Theta(\theta, \phi_0)$ and (right) $\Phi(\theta, \phi_0)$ versus θ for fixed values of ϕ ($\phi_0 = 20°$, $\phi_0 = 40°$, $\phi_0 = 60°$, and $\phi_0 = 80°$). The first-order results were obtained from equation 38a.

Finally, we consider the results for the fast qS-waves shown in Figure 7. Inspecting the $\Theta(\theta,\phi_0)$ plots, we note that in the domain $0 < \theta < 25°$, the deviation between the direction of the fast qS-wave group velocity and the wave vector can be as large as 20°, while the corresponding error never exceeds 3°. Moreover, referring to the azimuthal graphs $\Phi(\theta,\phi_0)$, we note that for the same propagation directions $0 < \theta < 25°$, the differences between first-order and exact results are negligible for all ϕ values. Thus, the first-order fast qS-wave group-velocity expression gives very accurate results for prevailingly vertical propagation directions. For propagation directions away from the vertical ($30° < \theta < 90°$), first-order fast S-wave results are shifted with respect to exact results and are less reliable.

As the analytic form of the approximate qS-wave group-velocity expressions predicts, these expressions are inaccurate for propagation near singular S-wave directions. This is evident in the fast qS-wave group-velocity azimuthal direction plot corresponding to $\phi = 40°$ (Figure 7). We see that in the domain $40° < \theta < 50°$, the exact graph for $\Phi(\theta,40°)$ undergoes a change of nearly 125° while going through a minimum. Here, the first-order approximation completely breaks down. This domain is near the qS-wave degenerate direction, located at $(\theta,\phi)_{\text{exact}} = (46.5°, 44.9°)$.

In summary, the derived first-order group-velocity expressions provide very good results for propagation directions tending toward the vertical. The numerical results from the Schoenberg and Helbig model show that the accuracy of our approximate group-velocity expressions is mode dependent. Letting $\theta_{\max}$ denote the upper bound for the near-vertical propagation directions ($0 < \theta < \theta_{\max}$) for which the errors in the first-order group-velocity polar and azimuthal directions do not exceed 3°, we can summarize our findings for each mode: For qP-waves, $\theta_{\max} = 50°$; for slow qS-waves, $\theta_{\max} = 40°$; and for fast qS-waves, $\theta_{\max} = 25°$. We have also observed that near qS-wave degenerate directions, first-order qS-wave group-velocity expressions cannot be expected to yield accurate results.

DISCUSSION AND CONCLUSIONS

The WCS has distinct advantages for deriving and expressing perturbation-theory formulas for qP and qS-wave phase velocities, group-velocity vectors, and polarization vectors. For a specified wave-propagation direction in an arbitrarily anisotropic medium, exact solutions of the Christoffel equation depend on only six WCS stiffness components. Based on this simplification of the Christoffel equation in the WCS and that for an isotropic medium the Christoffel matrix in the WCS is strictly diagonal, we conclude that the WCS is a natural coordinate system for the application of perturbation theory and the study of weak anisotropy.

For weakly anisotropic media, the off-diagonal components of the Christoffel matrix in the WCS are small (first-order) terms compared to the diagonal components. Moreover, in weakly anisotropic media, qP- and qS-waves may be treated, approximately, as longitudinal and transverse waves, respectively. These observations facilitate the order-of-magnitude analysis involved in our treatment of the perturbation-theory solution to the Christoffel equation, reducing it to simple algebraic manipulations. We treat the zero-order and first-order qS-wave polarization corrections under the same footing as angles by which the polarization directions are rotated about the wave vector. This facilitates the visualization of polarization orientations.

The economy in the number of independent stiffness components involved in the Christoffel matrix in the WCS, contributes to the conciseness of our general approximate wave-attribute expressions. They are displayed as linear functions of the stiffness components in the WCS, making the physical meaning of the terms of our expressions transparent. Using the example of orthorhombic symmetry, we illustrate how to transform the general wave-attribute expressions from the WCS to the acquisition coordinate system. We present these results as linear functions of the weak-anisotropy (orthorhombic) parameters; thus, the dependence of the presented expressions on the degree of anisotropy is apparent.

Using the Schoenberg and Helbig orthorhombic model, we illustrate the accuracy of the zero-order and first-order polarization expressions. Test results show that the precision of the derived approximate qS-wave polarization expressions increases as the propagation direction approaches the vertical. In the domain $0 < \theta < 40°$ and for all azimuth angles, the error in the zero-order approximation of the qS-wave polarization direction remains less than 5°, whereas the error in the first-order approximation is less than 3°. As expected, the first-order qS-wave polarization expressions are generally more accurate than the zero-order expressions. However, in light of its simplicity, the zero-order expressions may still be useful in processing data from weakly anisotropic geologic regions. The approximate qS-wave polarization expressions are unreliable near degenerate propagation directions.

The qP- and qS-wave group-velocity expressions developed in this paper for the general weakly anisotropic media complement previously published theoretical work on weak anisotropy. They can be incorporated into computer programs for forward and inverse modeling in weakly anisotropic elastic media and can be useful for computing traveltime tables in Kirchhoff migration that require ray tracing. As our group-velocity expressions show, while for weak anisotropy the difference between the magnitudes of phase velocity and group velocity can at most be a second-order quantity, the direction of the group velocity differs from the direction of the wave vector by a first-order amount. To illustrate the effect of anisotropy on group velocity directions, we use the Schoenberg and Helbig orthorhombic model, to generate plots of the polar and azimuthal angular deviations of the group-velocity directions from the wave-vector direction. The polar angle Θ gives the angle between the group-velocity vector and the wave vector, and it sufficiently describes the deviation angle in a homogeneous anisotropic medium. Numerical results show that the angular deviation for qP-waves can be as large as $\Theta_{\max} \approx 16°$. For the slow qS-waves, the corresponding maximum deviation angle is $\Theta_{\max} \approx 30°$ and for the fast qS-wave $\Theta_{\max} \approx 20°$. In light of these numbers, it is evident that when rays are traced across anisotropic interfaces and over large distances, their trajectories can diverge significantly from the direction of the wave vector.

Differences between the first-order and exact group-velocity plots provide a measure of the errors in the derived approximate expressions. Test results from the Schoenberg and Helbig model show that, for near-vertical propagations, the range of propagation directions (wave-vector direction θ) for which the errors do not exceed 3° depends on the particular wave mode. For qP-waves, slow qS-waves, and fast qS-waves, these ranges are $0 < \theta < 50°$, $0 < \theta < 40°$, and $0 < \theta < 25°$, respectively. The numerical results also confirm our prediction that the first-order qS-wave group-velocity expressions are unreliable in the vicinity of S-wave degeneracy.

The Schoenberg and Helbig orthorhombic model, with greater than 30% anisotropy, provides a robust test of the perturbation-theory results discussed in this paper. Numerical results show that the precision of the derived approximate expressions is high, even when anisotropy is strong. We have tested the derived approximate expressions against weaker models, generated by uniformly reducing the weak-anisotropy parameters of the Schoenberg and Helbig model. As expected, we find that when the anisotropy is weakened, the agreement between the first-order and the exact results improves.

ACKNOWLEDGMENT

We wish to thank ENSCO, Inc. for supporting this work and its publication.

APPENDIX A

TRANSFORMATION OF STIFFNESS COMPONENTS FROM WCS TO ACQUISITION COORDINATE SYSTEM

Using Voigt notation, any stiffness component C'_{rs} in the WCS may be expressed in terms of the stiffness components C_{ij} in the acquisition coordinate system and the wave-vector direction angles θ and ϕ by the relation

$$C'_{rs} = M_{ri}M_{sj}C_{ij} \text{ (sum over } i \text{ and } j \text{ from 1 to 6)}, \tag{A-1}$$

where the 6×6 Bond matrix $\mathbf{M}$ is explicitly given by

$$\mathbf{M} = \begin{bmatrix} C_\theta^2 C_\phi^2 & C_\theta^2 S_\phi^2 & S_\theta^2 & -S_{2\theta}S_\phi & -S_{2\theta}C_\phi & C_\theta^2 S_{2\phi} \\ S_\phi^2 & C_\phi^2 & 0 & 0 & 0 & -S_{2\phi} \\ S_\theta^2 C_\phi^2 & S_\theta^2 S_\phi^2 & C_\theta^2 & S_{2\theta}S_\phi & S_{2\theta}C_\phi & S_\theta^2 S_{2\phi} \\ -\frac{1}{2}S_\theta S_{2\phi} & \frac{1}{2}S_\theta S_{2\phi} & 0 & C_\theta C_\phi & -C_\theta S_\phi & S_\theta C_{2\phi} \\ \frac{1}{2}S_{2\theta}C_\phi^2 & \frac{1}{2}S_{2\theta}S_\phi^2 & -\frac{1}{2}S_{2\theta} & C_{2\theta}S_\phi & C_{2\theta}C_\phi & \frac{1}{2}S_{2\theta}S_{2\phi} \\ -\frac{1}{2}C_\theta S_{2\phi} & \frac{1}{2}C_\theta S_{2\phi} & 0 & -S_\theta C_\phi & S_\theta S_\phi & C_\theta C_{2\phi} \end{bmatrix}. \tag{A-2}$$

Here, we use the abbreviations $C_\theta = \cos\theta$, $S_{2\phi} = \sin 2\phi$, $S_\theta^2 = \sin^2\theta$, etc.

For a discussion of the general form of the Bond matrix $\mathbf{M}$ for transforming stiffness components between any two Cartesian coordinate systems, see section 3.D of Auld (1973).

APPENDIX B

ABREVIATIONS USED IN ORTHORHOMBIC EXPRESSIONS

Following are the explicit expressions for the abbreviations used in the derived first-order formulas for weak orthorhombic media. Only terms linear in the weak-anisotropy parameters g_{ij} are retained.

$$\begin{aligned} P(\theta,\phi) = \sin^2\theta[&\sin^2\theta(g_{11}\cos^4\phi + g_{22}\sin^4\phi \\ &+ g_{12}\cos^2\phi\sin^2\phi) + \cos^2\theta(g_{23}\sin^2\phi \\ &+ g_{13}\cos^2\phi)], \end{aligned} \tag{B-1}$$

$$\begin{aligned} S(\theta,\phi) = \frac{C_{33}}{2C_{44}}\sin^2\theta\{&g_{11}\cos^2\phi(\cos^2\phi\cos^2\theta + \sin^2\phi) \\ &+ g_{22}\sin^2\phi(\sin^2\phi\cos^2\theta + \cos^2\phi) \\ &- \cos^2\theta(g_{23}\sin^2\phi + g_{13}\cos^2\phi) \\ &- g_{12}\sin^2\theta\sin^2\phi\cos^2\phi\} \\ &+ \left(\frac{1}{2}\right)[g_{55}(1 - \sin^2\phi\sin^2\theta) + g_{66}\sin^2\theta]. \end{aligned} \tag{B-2}$$

$$\begin{aligned} M(\theta,\phi) = \frac{C_{33}}{2C_{44}}\sin^2\theta\{&g_{11}\cos^2\phi(\cos^2\phi\cos^2\theta - \sin^2\phi) \\ &+ g_{22}\sin^2\phi(\sin^2\phi\cos^2\theta - \cos^2\phi) \\ &- \cos^2\theta(g_{23}\sin^2\phi + g_{13}\cos^2\phi) \\ &+ g_{12}(1 + \cos^2\theta)\sin^2\phi\cos^2\phi\} \\ &+ \left(\frac{1}{2}\right)[g_{55}(\cos^2\phi - \sin^2\phi\cos^2\theta) \\ &- g_{66}\sin^2\theta], \end{aligned} \tag{B-3}$$

$$\begin{aligned} N(\theta,\phi) = \frac{\sin 2\phi\cos\theta}{4}\Bigg[&\frac{C_{33}}{C_{44}}\sin^2\theta(-2g_{11}\cos^2\phi \\ &+ 2g_{22}\sin^2\phi - g_{23} + g_{13} + g_{12}\cos 2\phi) - 2g_{55}\Bigg], \end{aligned} \tag{B-4}$$

$$\begin{aligned} A(\theta,\phi) = \frac{\sin 2\theta}{2\left(1 - \frac{C_{44}}{C_{33}}\right)}\Bigg[&2\sin^2\theta(g_{11}\cos^4\phi + g_{22}\sin^4\phi) \\ &+ \cos 2\theta(g_{23}\sin^2\phi + g_{13}\cos^2\phi) \\ &+ \frac{1}{2}g_{12}\sin^2 2\phi\sin^2\theta\Bigg], \end{aligned} \tag{B-5}$$

$$\begin{aligned} B(\theta,\phi) = \frac{\sin 2\phi\sin\theta}{2\left(1 - \frac{C_{44}}{C_{33}}\right)}&[2\sin^2\theta(-g_{11}\cos^2\phi + g_{22}\sin^2\phi) \\ &+ \cos^2\theta(g_{23} - g_{13}) + g_{12}\cos 2\phi\sin^2\theta], \end{aligned} \tag{B-6}$$

$$F_1(\theta,\phi) = v_s^0\frac{\sin 2\theta}{2}\Bigg\{-\frac{C_{33}}{C_{44}}\Bigg[g_{11}\cos^2\phi(2\cos^2\phi\sin^2\theta - 1) + g_{22}\sin^2\phi(2\sin^2\phi\sin^2\theta - 1) + \cos 2\theta(g_{23}\sin^2\phi + g_{13}\cos^2\phi) + \frac{1}{2}g_{12}\sin^2 2\phi\sin^2\theta\Bigg] - g_{55}\sin^2\phi + g_{66}\Bigg\}, \quad \text{(B-7)}$$

$$G_1(\theta,\phi) = v_s^0\frac{\sin 2\theta}{2}\Bigg\{\frac{C_{33}}{C_{44}}\Bigg[g_{11}\cos^2\phi(2\cos^2\phi\cos^2\theta - 1) + g_{22}\sin^2\phi(2\sin^2\phi\cos^2\theta - 1) - \cos 2\theta(g_{23}\sin^2\phi + g_{13}\cos^2\phi) + \frac{1}{2}g_{12}\sin^2 2\phi\cos^2\theta\Bigg] + g_{55}\sin^2\phi - g_{66}\Bigg\}, \quad \text{(B-8)}$$

$$H_1(\theta,\phi) = v_s^0\frac{\sin 2\phi\sin\theta}{4}\Bigg\{\frac{C_{33}}{C_{44}}(3\cos^2\theta - 1) \times[-2g_{11}\cos^2\phi + 2g_{22}\sin^2\phi - g_{23} + g_{13} + g_{12}\cos 2\phi] + 2g_{55}\Bigg\}, \quad \text{(B-9)}$$

$$F_2(\theta,\phi) = v_s^0\frac{\sin 2\phi\sin\theta}{2}\Bigg\{\frac{C_{33}}{C_{44}}[g_{11}(2\cos^2\phi\sin^2\theta - 1) - g_{22}(2\sin^2\phi\sin^2\theta - 1) + (g_{13} - g_{23})\cos^2\theta - g_{12}\cos 2\phi\sin^2\theta] - g_{55}\Bigg\}, \quad \text{(B-10)}$$

$$G_2(\theta,\phi) = v_s^0\frac{\sin 2\phi\sin\theta}{2} \times\left[\frac{C_{33}}{C_{44}}\cos 2\phi(g_{12} - g_{11} - g_{22}) - g_{55}\right], \quad \text{(B-11)}$$

$$H_2(\theta,\phi) = v_s^0\frac{\sin 2\theta}{4}\Bigg\{\frac{C_{33}}{C_{44}}\Bigg[2g_{11}\cos^2\phi(2\sin^2\phi - \cos^2\phi\sin^2\theta) + 2g_{22}\sin^2\phi(2\cos^2\phi - \sin^2\phi\sin^2\theta) + g_{23}(2\sin^2\phi\sin^2\theta - 1) + g_{13}(2\cos^2\phi\sin^2\theta - 1) + g_{12}\left(\cos^2 2\phi - \frac{1}{2}\sin^2 2\phi\sin^2\theta\right)\Bigg] + 2g_{55}\sin^2\phi - 2g_{66}\Bigg\}. \quad \text{(B-12)}$$

REFERENCES

Auld, B. A., 1973, Acoustic waves and fields in solids: John Wiley & Sons, Inc.

Backus, G. E., 1965, Possible forms of seismic anisotropy of uppermost mantel under oceans: Journal of Geophysical Research, **70**, 3429–3439.

Byun, B. S., and D. Corrigan, 1990, Seismic traveltime inversion for transverse isotropy: Geophysics, **55**, 192–200.

Carcione, J. M., 2001, Wave fields in real media: Wave propagation in anisotropic, anelastic and porous media: Handbook of Geophysical Exploration, **31**, Pergamon Press.

Cheadle, S., R. Brown, and D. Lawton, 1991, Orthorhombic anisotropy: A physical seismic modeling study: Geophysics, **56**, 1603–1613.

Faria, E. L., and P. L. Stoffa, 1994, Traveltime computation in transversely isotropic media: Geophysics, **59**, 272–281.

Farra, V., and I. Pšenčík, 2003, Properties of the zeroth-, first-, and higher-order approximations of attributes of elastic waves in weakly anisotropic media: Journal of the Acoustical Society of America, **114**, 1366–1378.

Gajewski, D., and I. Pšenčík, 1996, qP-wave phase velocities in weakly anisotropic media — Perturbation approach: 66th Annual International Meeting, SEG, Expanded Abstracts, 1507–1510.

Igel, H., P. Mora, and D. Rodrigues, 1991, Modeling anisotropic waves in three dimensions: 53rd Annual Meeting, EAEG, Extended Abstracts, 558–559.

Jech, J., and I. Pšenčík, 1989, First-order perturbation method for anisotropic media: Geophysical Journal International, **99**, 369–376.

Landau, L. D., and E. M. Lifschitz, 1977, Quantum mechanics — Non-relativistic theory: Pergamon Press.

Mensch, T., and P. Rasolofosaon, 1997, Elastic-wave velocities in anisotropic media of arbitrary symmetry — Generalization of Thomsen's parameters ε, δ and γ: Geophysical Journal International, **128**, 43–64.

Ohanian, V., 1996, Weak transverse isotropy by perturbation theory: 66th Annual International Meeting, SEG, Expanded Abstracts, 1838–1841.

Ohanian, V., T. M. Snyder, and J. M. Carcione, 1997, Mesaverde and Green River Shale anisotropies by wavefront folds and interference patterns: 67th Annual International Meeting, SEG., Expanded Abstracts, 937–940.

———, 2002, Explicit imaging expressions for weak horizontal transverse isotropy: 72nd Annual International Meeting, SEG, Expanded Abstracts, 153–156.

Pšenčík, I., and D. Gajewski, 1998, Polarization, phase velocity, and NMO velocity of qP-waves in arbitrary weakly anisotropic media: Geophysics, **63**, 1754–1766.

Rommel, B. E., 1994, Approximate polarization of plane waves in a medium having weak transverse isotropy: Geophysics, **59**, 1605–1612.

Sayers, C. M., 1994, P-wave propagation in weakly anisotropic media: Geophysical Journal International, **116**, 799–805.

Schoenberg, M., and K. Helbig, 1997, Orthorhombic media: Modeling elastic wave behavior in a vertically fractured earth: Geophysics, **62**, 1954–1974.

Symon, K. R., 1971, Mechanics, 3rd ed.: Addison-Wesley Publishing Company.

Thomsen, L., 1986, Weak elastic anisotropy: Geophysics, **51**, 1954–1966.

Thomson, C. J., J. M. Kendall, and W. S. Guest, 1992, Geometrical theory of shear wave splitting: Corrections to ray theory for interference in isotropic/anisotropic transitions: Geophysical Journal International, **108**, 339–363.

Tsvankin, I., 1997, Anisotropic parameters and *P*-wave velocity for orthorhombic media: Geophysics, **62**, 1292–1309.

Wolfe, J. P., and M. R. Hauser, 1995, Acoustic wavefront imaging: Annalen der Physik, **4**, 99–126.